ARMY RESEARCH LABORATORY

Comparative Studies of Polymer Electrolyte Membrane Fuel Cell Stacks and Single Cells

Deryn Chu and Rongzhong Jiang

ARL-TR-2087 February 2000

The findings in this report are not to be construed as an official Department of the Army position unless so designated by other authorized documents.

Citation of manufacturer's or trade names does not constitute an official endorsement or approval of the use thereof.

Destroy this report when it is no longer needed. Do not return it to the originator.

Army Research Laboratory

Adelphi, MD 20783-1197

ARL-TR-2087 **February 2000**

Comparative Studies of Polymer Electrolyte Membrane Fuel Cell Stacks and Single Cells

Deryn Chu and Rongzhong Jiang

Sensors and Electron Devices Directorate

Abstract

We made a comparative investigation of a polymer electrolyte membrane fuel cell (PEMFC) with a single cell and a 30-cell stack. Various types of Nafion membranes, such as Nafion 102, 112, 115, and 117, and 105, were tested as electrolytes with the single cell at different temperatures. Nafion 112 gave us the optimal result. We evaluated the 30-cell stack at different temperatures and humidity levels. The potential-current and power-current curves for both the single cell and the stack were analyzed by computer simulation, during which the kinetic and mass-transfer parameters were calculated. We also measured the performance of the stack and its water production during long-term operation.

Contents

Figures

Tables

1. Introduction

Because of its light weight and high-energy, high-power, nonemissive, and low-temperature operation, the polymer electrolyte membrane fuel cell (PEMFC) has received much attention in recent years [1–10]. The research and development of materials, catalysts, and electrode components for the single-cell PEMFC has seen significant progress during the past several decades. To meet the requirements for practical applications, a large number of single cells, known as a PEMFC stack, are assembled together. Recently, many PEMFC stacks of a variety of types and functions have been developed [11–14]. The performance of a PEMFC stack is different from that of a single PEMFC. The PEMFC stack has a much higher operating voltage and is more powerful and energy efficient. In this report, we explore differences in the electrochemical performance between PEMFC stacks and single cells, and attempt to accelerate the practical military and civilian applications of PEMFC stacks as portable power sources. For the single cell, we emphasize the important role of different Nafion membranes in the construction of the membrane electrode assembly (MEA) of PEMFCs. For the stack, we evaluate the performance of a 100-W PEMFC stack that consists of 30 cells, with an emphasis on kinetic and mass-transfer electrode processes.

2. Experimental

2.1 PEMFC Stack

The subject of our experiment was a self-humidifying 100-W PEMFC stack made up of 30 cells connected in a series. The area of each electrode was approximately 60 cm^2, and the open-circuit voltage was approximately 30 V. We supplied air to the cathode by an electric fan, and used another electric fan for cooling the stack. A self-humidifying function was obtained by the blowing of air through a small chamber where water was collected from the stack's cathodes. High-purity hydrogen (99.99%) was used. The environmental temperature and humidity of the stack were controlled with a Tenney environment chamber (model BTRC) (which was programmed through a computer with Linktenn II software) and a Heatless dryer (model HF 200A). An Arbin battery tester (model BT-2043) was used for computer-controlled experiments for the PEMFC stack test. To get reproducible results, we carried out all the varying temperature experiments within the Tenney environment chamber for the PEMFC stack after constant temperature and humidity had been maintained for more than 6 hr.

2.2 PEMFC Single Cell

Various Nafion membranes (numbered 105, 112, 115, and 117) were obtained from the DuPont Chemical Company. We soaked them in an H_2O_2/H_2O solution at about 80 °C for 2 hr. After the Nafion membranes became transparent, we washed them with distilled water. We then soaked and boiled them in a 1-M H_2SO_4 solution for 2 hr, and rinsed them in water to remove excess H_2SO_4. The membranes were then stored in distilled water until we were ready to use them. The commercially available electrocatalyst, 20% platinum on Vulcan XC-72 carbon (from E-Tek), was suspended in an aqueous Nafion solution. The mixture was then sonicated in an ultrasonic bath. The final electrocatalyst-Nafion mixture was sprayed onto Tory carbon paper. The amounts of Pt and Nafion on the electrode were about 0.4 and 0.5 mg/cm^2, respectively. The MEA, a key component of the PEMFC system, is a proton-conducting membrane such as Nafion, laminated between the active sites of two electrodes (carbon-supported Pt black). MEA is conventionally assembled by a hot pressing process conducted at 140 °C and 1200 psi for 90 s. During this process, the electrode-membrane-electrode laminate is heated until the glass transition temperature of the membrane is reached. We used two titanium plates with fine gas-passing channels with their inner sides to the MEA to hold the MEA as a single cell. Pure hydrogen was the fuel and pure oxygen was the oxidant. We used a Hewlett-Packard electronic load (model 6050A) and a Hewlett-Packard multimeter to measure the single cell's current and voltage, respectively.

3. Results and Discussion

3.1 Performance of a Single Cell

3.1.1 Effect of Nafion Membrane

Figure 1 shows the polarization curves of a single-cell PEMFC with different MEAs. These results are typical of hydrogen-oxygen fuel cells. The initial drop of the potential-current curve is due to an electrochemical activation process, which is caused by the sluggish kinetics of oxygen reduction at the cathode-electrode surface. The linear decrease of the potential-current curves with increasing load-current density is due to ohmic polarization, which is attributed to the ion flow through the electrolyte membrane and the electron flow through the electrode materials. These results demonstrate that the current density is significantly enhanced when the membrane thickness is decreased from 7 mil (Nafion 117) to 2 mil (Nafion 112). For Nafion membranes 112, 105, 115, and 117, the values of the current density of the single cell at 0.72 V are about 1.0, 0.6, 0.5, and 0.4 A/cm^2, respectively. Apparently, the Nafion 112

membrane offers the optimal performance. The kinetic parameters can be obtained by computer simulation with the following empirical equations:

$$E_i = E_o - b \log i - Ri \ , \tag{1}$$

$$E_o = E_r + b \log i_o \ , \tag{2}$$

$$E_i = E_o - b \log i - Ri - i_m m \exp[ni_m] \ , \tag{3}$$

$$i_m = i - i_d \text{ (when } i > i_d) \ , \text{ and} \tag{4}$$

$$i_m = 0 \text{ (when } i \leq i_d) \ . \tag{5}$$

Here, E_i and i are the measured potential and current experimentally, E_r is the reversible potential for the cell, and i_o and b are the exchange current and the Tafel slope for the oxygen reduction, respectively. R represents the dc resistance, such as the resistance of the polymer membrane and other electrode components, that causes the linear variation of potential with current as mentioned above. In addition, m and n are the mass-transfer parameters. Here, the i_d is the minimum value of current that causes the voltage deviation from the linearity at the higher current range. The i_d value can be obtained from the experimental curve and from the calculated curve with equation (1). Hence, equation (1) can be used to describe the electrochemical process, which is controlled only by activation and ohmic processes, while equation (3) can be used to describe the entire electrochemical process including activation, ohmic, and mass-transfer controls.

For the conditions of Nafion membranes 105, 112, and 115, there is no apparent mass-transfer process: no deviation from linearity was observed at the high-current range on these curves. However, when Nafion 117 was used as the membrane, the curve was bent down slightly at the high current-density range. Apparently, this bend signals the existence of a mass-transfer process. In figure 1, the points were obtained from experiments and the lines were simulated from equation (1) (for Nafions 105, 112, and 115) or from equation (3) (for Nafion 117). The single cell's kinetic and mass-transfer parameters for different Nafion membranes are shown in table 1. The E_o value shows no significant change for different Nafion membranes. It is interesting that the b and R values decrease in the order of Nafions 117, 115, 105, and 112. The power-current curves are also shown in figure 1. A peak power is observed at about 0.9 A/cm^2 on the power-current curve for Nafion 117. For other Nafion membranes, no peak power is observed. The simulated curves can be used to predict the single cell's performance beyond the experimental points. For example, at 1.2 A/cm^2, the power densities for Nafions 112, 105, 115, and 117 are estimated at 0.82, 0.68, 0.61, and 0.23 W/cm^2, respectively.

Table 1. Electrode kinetic and mass-transfer parameters calculated from polarization curves for single PEMFC with different Nafion electrolyte membranes at 50 °C.

Nafion No.	E_o (V)	b (mV/dec)	R ($\Omega \cdot cm^2$)	m ($\Omega \cdot cm^2$)	n (cm^2/A)	i_d ($A \cdot cm^{-2}$)
112	0.99	56.0	0.11	—	—	—
105	1.00	58.0	0.21	—	—	—
115	1.01	62.0	0.26	—	—	—
117	1.02	68.0	0.33	0.18	0.15	0.65

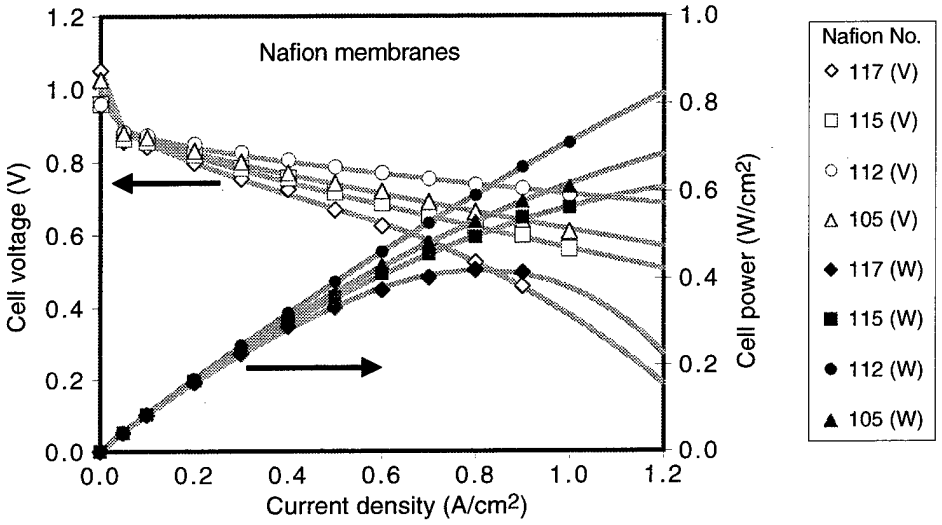

Figure 1. Polarization curves of single cell with various MEAs. Points are experimental data and lines are from simulation with an empirical equation.

3.1.2 *Effect of Temperature*

Because of its optimal performance, the Nafion 112 membrane was selected for further study in the temperature experiment. Figure 2 shows the potential-current and power-current curves for the Nafion 112 membrane as an MEA at various temperatures. Usually, a single cell has good heat exchange performance with the environment. Therefore, the inner temperature and the environmental temperature can be considered the same for the single cell (this is not the case for the stack). The single cell's potential increases with temperature from 24 to 50 °C, as does the power for the same current density condition. At higher temperatures the ionic conductivity of the Nafion membrane is enhanced and the rate of the electrode reactions is faster at both electrodes. It seems that higher temperatures would be better for the operation of a single cell. However, further temperature increases would cause dehydration of the membrane, resulting in reduced conductivity and inferior cell performance. The simulated curves in figure 2 show that the cell voltage at a current density of 1.4 A/cm^2 is 0.51, 0.60, and 0.66 V at 24, 40, and 50 °C, respectively. The power at the same current density is 0.72, 0.84, and 0.92 W/cm^2. The electrode-kinetic parameters for the single cell using Nafion 112 as the membrane at different temperatures are summarized in table 2. The parameters of b and E_o seem to show no significant difference. However,

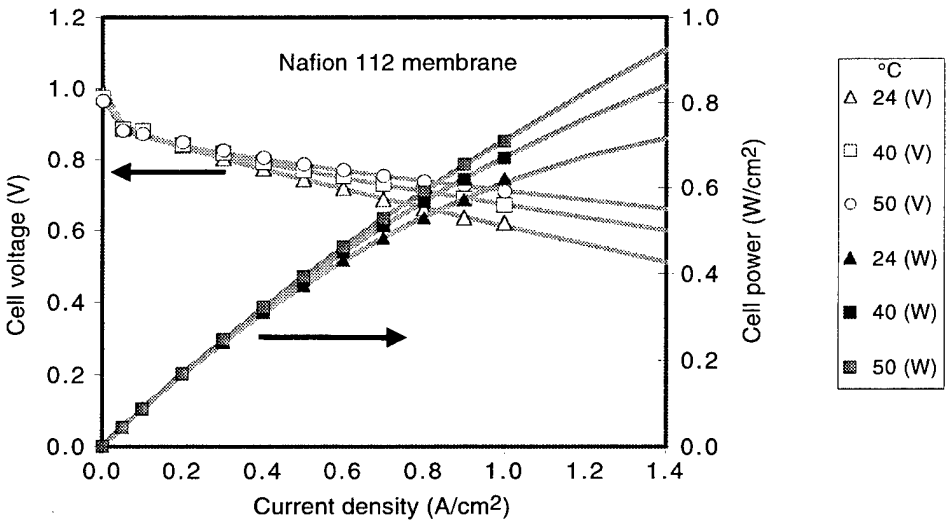

Figure 2. Electrochemical performance of Nafion 112 MEAs at various temperatures. Points are experimental data and lines are from simulation with an empirical equation.

Table 2. Electrode kinetic parameters calculated from polarization curves for single PEMFC with Nafion 112 as electrolyte membrane at different temperatures.

Temperature (°C)	E_o (V)	R ($\Omega \cdot cm^2$)	b (mV/dec)
24	1.01	0.23	56.0
40	1.00	0.16	56.0
50	0.99	0.11	56.0

R gets smaller with an increase of temperature because the ionic conductance of the membrane electrolyte is improved at the elevated temperatures.

3.2 Performance of PEMFC Stack

3.2.1 General polarization curves

Figure 3 shows the potential-current and power-current curves of a 30-cell 100-W PEMFC stack at room temperature (about 20 °C) and room humidity conditions (about 70% RH). The shape of both curves is not much different from those of the single cell, except for the much higher open-circuit potential (about 30 times that of the single cell) and much higher power output. The points on the curves were obtained from the experiment, and the lines were obtained from the simulation with equation (1). Up to a current of 7 A, there is no apparent curving down as observed on the potential-current curve, and the data fit with equation (1) is good. The electrode process is of activation and ohmic control within this current range. Because the stack is made up of 30 cells, heat equilibrium inside the stack is hard to reach. Therefore, the temperature gradient across the interior of the stack to the environment is significant and is also time-dependent. This feature makes the evaluation of the PEMFC stack more

difficult than that of a single cell. Also, because heat produced at the inner stack cannot dissipate quickly, the inside and outside temperature of the stack may vary up to more than 26 °C, depending on different experimental conditions. At a current of 7 A, the voltage and power of the stack are 19.8 V and 140 W, respectively. From the simulated curves, one can see that if the current is extended to 10 A, the voltage and power will be 18.3 V and 183 W, respectively. The electrode kinetic parameters are also obtained from the simulation, and these are shown in the last row in table 3. Here, the value of E_o, b, or R should be the sum of the values of all the single cells: i.e., 30 times that of the average of a single cell. Therefore, for each single cell the average values of E_o, b, and R are 1.07 V, 83 mV/dec, and 0.013 Ω, respectively. Surprisingly, with the designed 30-cell 100-W PEMFC stack, we obtained more than 140 W at a current of 7 A. The optimal performance of the stack can even reach 180 W at 10 A. These results demonstrate that the PEMFC stack offers more advantages than does a single cell.

3.2.2 *Effect of Humidity*

Although the 30-cell PEMFC stack is designed with a self-humidifying function, we still evaluated the effect of relative humidity (% RH) on the stack's performance. We placed the PEMFC stack into a Tenney environment chamber, where the temperature and humidity were controlled.

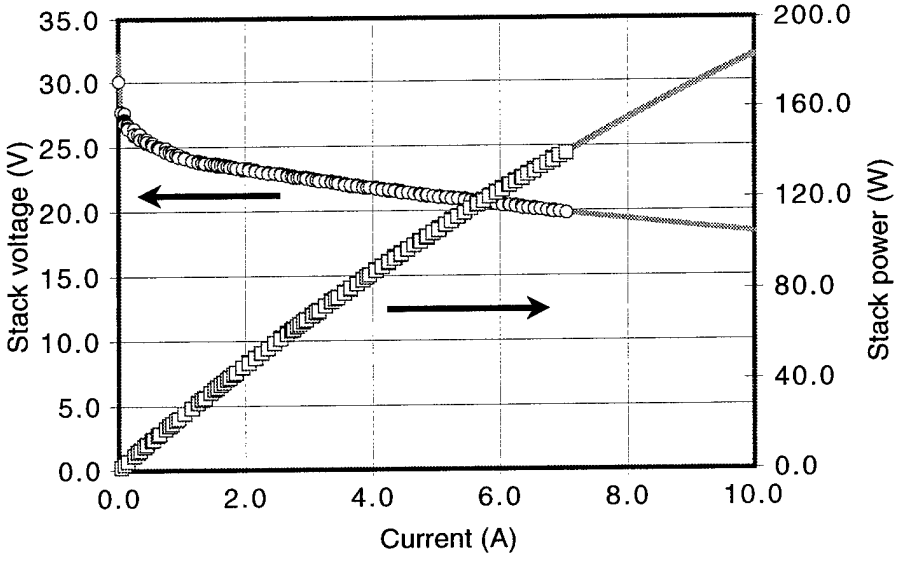

Figure 3. Polarization behavior of 30-cell 100-W PEMFC stack at room temperature (about 20 °C) and room humidity (about 70% RH) conditions. Points are experimental data and lines are from simulation with an empirical equation.

% RH	E_o (V)	b (mV/dec)	R (Ω)	m (Ω)	n (A^{-1})	i_d (A)
90	31.5	1900	0.37	0.31	0.15	4.54
10	31.0	1900	0.39	0.36	0.15	4.04
Room RH[a]	32.2	2500	0.39	—	—	—

[a]Room relative humidity: about 70% RH at room temperature (about 20 °C).

Table 3. Electrode kinetic and mass-transfer parameters for 30-cell 100-W PEMFC stack at different humidity levels. Temperature is constant at 30 °C.

Figure 4 shows the potential-current and power-current curves for the PEMFC stack with different humidity levels at a constant temperature of 30 °C. The relative humidity varies on the order of 10, 30, 50, 70, and 90% RH (for clarity, only 10 and 90% RH are included in fig. 4). As expected, the potential-current and power-current curves from 10 to 90% RH are only slightly different. Here, the self-humidifying function plays an important role. In figure 4, the potential-current curves bend down slightly at the higher current range. This indicates a mass-transfer process. Therefore, an excellent experimental data fit was obtained with equation (3). The simulated curves are lines shown in figure 4. Peak power is displayed on the power-current curves. The values of peak power at 10 and 90% RH are 146.0 W at 9.0 A and 167.4 W at 10.1 A, respectively. We obtained the kinetic and mass-transfer parameters from simulation, and these are shown in table 3. For the humidity change from 10 to 90% RH, the parameters of E_o, b, and R change only slightly. Here, the n value describes the degree of curvature on the potential-current curve at a higher current range. Under both conditions (10 and 90% RH), the n value is very small, about 0.15. The i_d value is larger and the m value is smaller at 90% RH than at 10% RH. Apparently, the stack performance at a higher humidity is less affected by the mass-transfer process.

The self-humidifying function in the PEMFC stack is less efficient with lower temperatures. We tested this assumption by keeping the temperature at 10 °C while varying the humidity. Each of the humidity experiments was separated by more than 6 hr, because self-heating occurred after each measurement, and this heating may have changed the temperature of the stack and caused poor reproducibility. Figure 5 shows the experimental potential-current and power-current curves for the PEMFC stack at different humidity levels and a constant temperature of 10 °C. As expected, the stack voltage on the potential-current curves decreases significantly with decreasing humidity. For example, at 25% RH the PEMFC stack cannot work properly: the open voltage decreases to only 18.6 V, the potential drops rapidly to 0 V, and the stack is out of power.

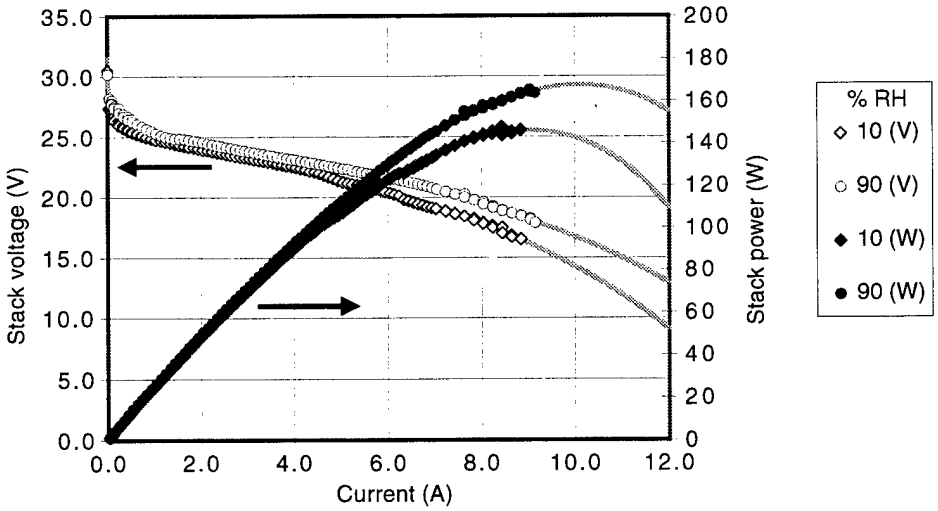

Figure 4. Effect of relative humidity on operating potential and power for 30-cell 100-W PEMFC stack at constant temperature of 30 °C. Points are experimental data and lines are from simulation with an empirical equation.

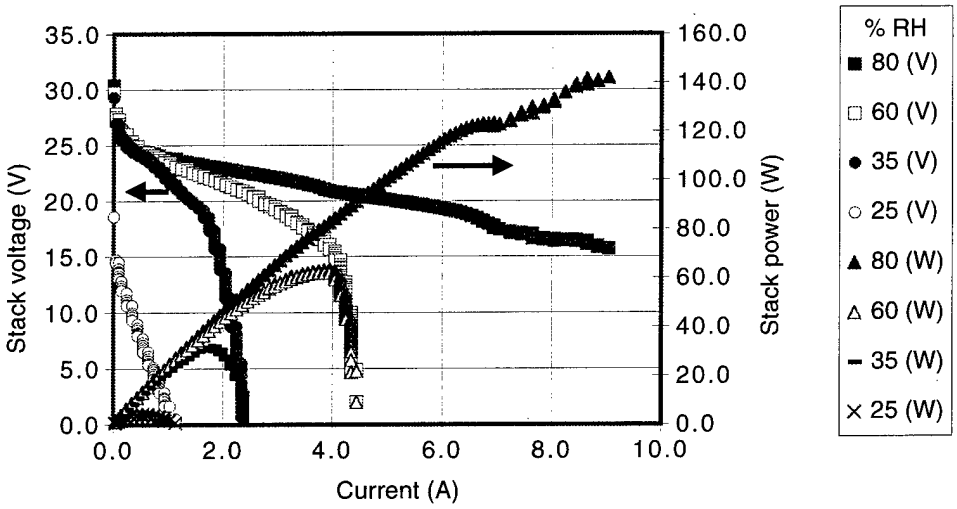

Figure 5. Effect of relative humidity on potential and power for 30-cell 100-W PEMFC stack at constant temperature of 10 °C.

Two humidity levels, 35 and 80% RH, were selected for electrode kinetic analysis. Figure 6 shows the simulation of potential-current and power-current curves at humidity levels of 35 and 80%. At a current lower than 6.5 A, the calculated curves and experimental data fit excellently for the 80% RH level. However, because self-heating occurred during the measurement and increased the stack's inner temperature, the calculated data do not agree with the experimental results when the current is greater than 6.5 A at 10 °C. For humidity levels of 80 and 35% RH, the values of peak power are 143.7 W at 9.9 A and 32.1 W at 1.85 A, respectively. The kinetic and mass-transfer parameters are obtained for different humidity levels at 10 °C and are shown in table 4. The R value at 35% RH is much greater than at 80% RH. Apparently, the low humidity causes the stack resistance to increase significantly at the low temperature. The n value is much greater, the i_d value is smaller, and the m value is greater at 35% RH than at 80% RH. These data indicate a poor mass-transfer process for low-humidity conditions at 10 °C. Why is the effect of humidity on the stack's performance more apparent at 10 °C than at 30 °C? Because it is more difficult for the accumulated H_2O to evaporate at lower temperatures. At temperatures below 10 °C, the air blown through the stack's chamber is hardly self-wetting and, as a result, the stack loses its self-humidifying function.

3.2.3 *Effect of Temperature*

Figure 7 shows the effect of temperature on the PEMFC stack's performance. To obtain reproducible results, we conducted each temperature experiment after the temperature was equilibrated for at least 6 hr. The initial rapid voltage drop in the very low current range on the potential-current curve stems from an electrode activation process, while the middle portion of the curve is controlled by an ohmic process. A slight mass-transfer behavior in these curves is observed in the higher current range. With an increase in current, the potential-current curves drop but the power-current curves rise. The highest power (about 165 W) is

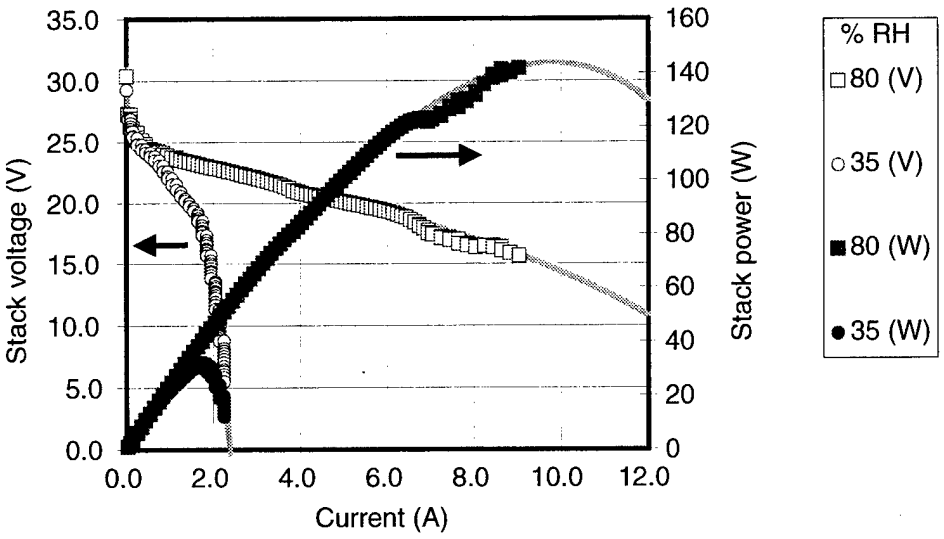

Figure 6. Effect of relative humidity on potential and power for 30-cell 100-W PEMFC stack at constant temperature of 10 °C. Points are experimental data and lines are from simulation with an empirical equation.

% RH	E_o (V)	b (mV/dec)	R (Ω)	m (Ω)	n (A^{-1})	i_d (A)
80	30.5	2050	0.48	0.19	0.15	3.64
35	31.0	2150	2.40	0.46	2.50	1.04

Table 4. Electrode kinetic and mass-transfer parameters for 30-cell 100-W PEMFC stack at different humidity levels. Temperature is constant at 10 °C.

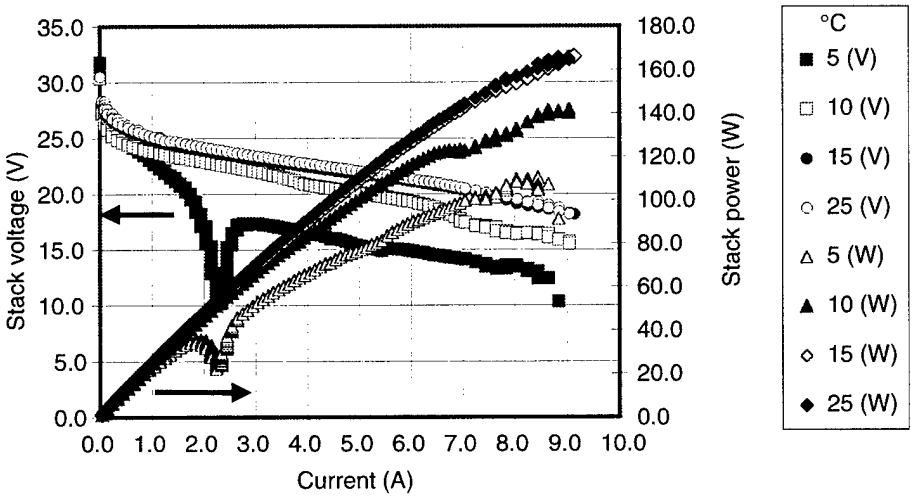

Figure 7. Effect of temperature on potential and power for 30-cell 100-W PEMFC stack at constant 80% RH.

obtained at about 9 A for a temperature of 15 or 25 °C. However, at low temperatures the potential-current and power-current curves are not smooth because the temperature of the inner stack fluctuated as the current passed through it. Especially at 5 °C, the inner stack warmed up significantly during the operation, causing the inner temperature to rise far above 5 °C. Therefore, the potential-current and power-current curves rise again significantly when the current is more than about 2.5 A. This phenomenon is attributed to the formation of a new heat-exchange balance system between the stack and the environment at the higher current range.

We completed the analysis of the electrode kinetic process by computer simulation. Figure 8 shows the simulated potential-current and power-current curves obtained from equation (3) at different temperatures. The lines and points in the figure represent the simulated curves and experimental data, respectively. For a temperature of 25 °C, all experimental points fit excellently. However, at 5 °C, only the initial part of the experimental data (current less than 2.5 A) shows a good fit. Peak power is displayed on these power-current curves. For temperatures of 25 and 5 °C, the values of peak power are 171.4 W at 10.6 A and 35.7 W at 1.95 A, respectively. The kinetic and mass-transfer parameters at different temperatures are shown in table 5. At lower temperatures, the R value is significantly larger, which reflects the decrease of ionic conductivity of the Nafion membrane. The i_d value is much smaller and the n value is much larger at 5 °C than at 25 °C. These results imply that a poorer mass-transfer process occurs at the lower temperature (5 °C).

3.2.4 *Performance for Long-Term Operation*

We evaluated the performance of the PEMFC for long-term operation. Figure 9 shows the plot of voltage versus time for the PEMFC stack at a constant current (7.0 A) discharge for 6 hr. For the first 4 hr, the voltage fluctuates. However, after 4 hr, the voltage remains constant at about 20 V. Because of many factors, such as electrode activation, heat exchange, mass-transfer, and humidifying, more time is required to reach the

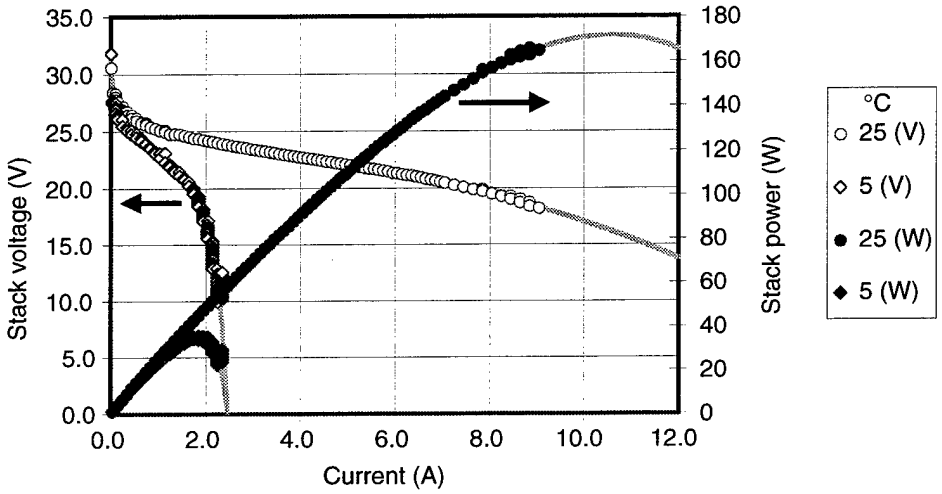

Figure 8. Effect of temperature on potential and power for 30-cell 100-W PEMFC stack at constant 80% RH. Points are experimental data and lines are from simulation with an empirical equation.

Table 5. Electrode kinetic and mass-transfer parameters for 30-cell 100-W PEMFC stack at different temperatures. Relative humidity is constant at 80% RH.

Temperature (°C)	E_o (V)	b (mV/dec)	R (Ω)	m (Ω)	n (A^{-1})	i_d (A)
25	32.0	2100	0.44	0.30	0.15	6.04
5	31.0	1900	2.40	0.22	3.50	1.25

equilibrium within the 30-cell PEMFC stack, and the optimal performance is obtained only after several hours of operation. Figure 10 shows a constant power (100-W) discharge performance for the PEMFC stack for 10 hr. After operating for about 3 hr, the system seems to become constant and the plot of voltage versus time is smooth. The two experiments described above demonstrate that the 30-cell PEMFC stack can work continuously for a long time. During long-term operation, much water was produced, which was continuously collected in the stack's chamber and removed for analysis. Figure 11 shows the water production during constant power discharge. Only about 66% theoretical water was collected. The rest of the water (34%) might be lost by evaporation and blown into the environment by the cooling and oxidant fans. The water blown out by the fans plays an important role in humidifying the PEMFC stack.

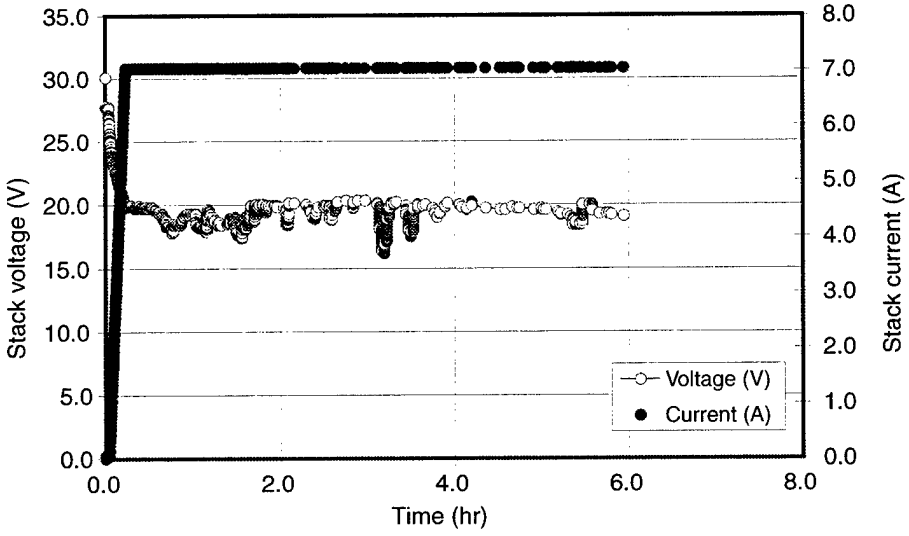

Figure 9. Constant current discharge performance of 30-cell 100-W PEMFC stack. At beginning, current was increased gradually then kept constant.

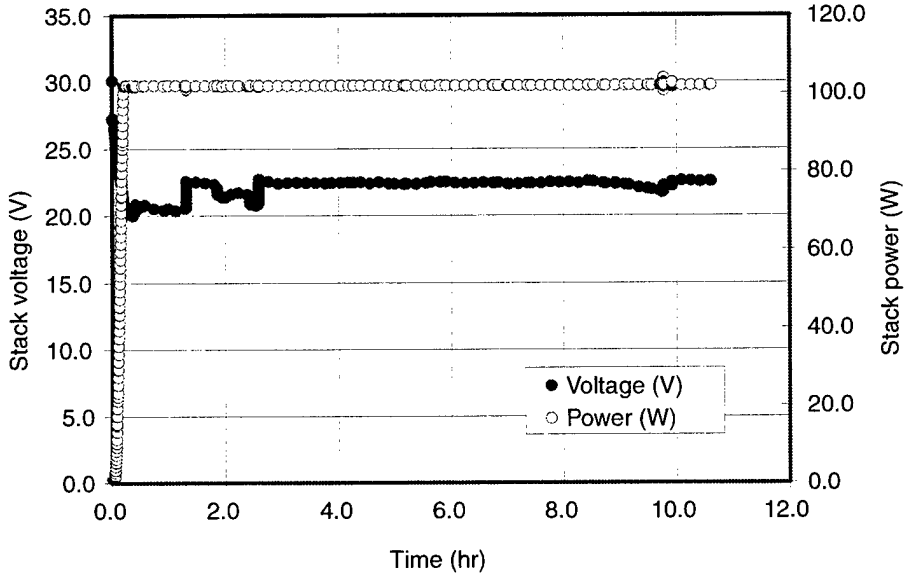

Figure 10. Constant power discharge performance of 30-cell 100-W PEMFC stack. At beginning, power was increased gradually to 100 W, then kept constant.

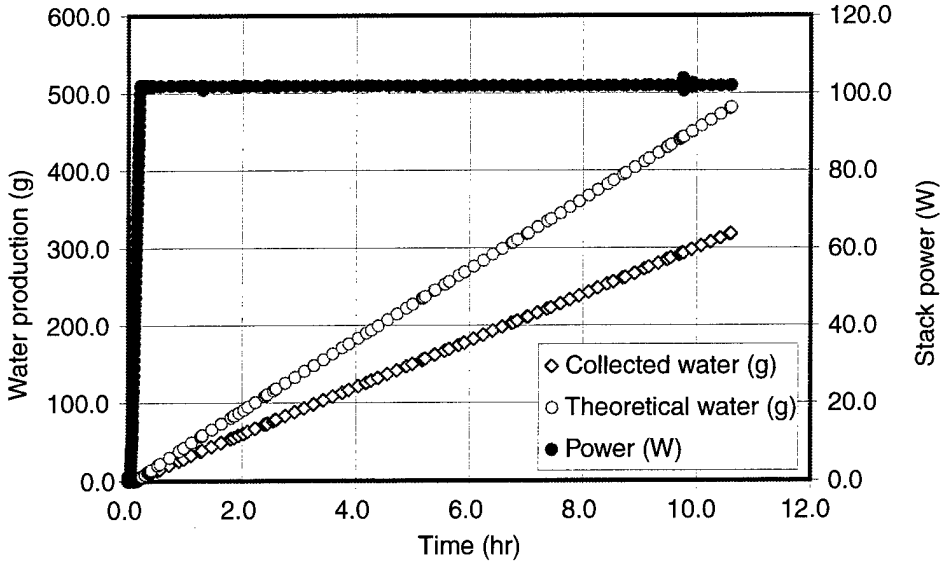

Figure 11. Water production during constant power discharge for 30-cell 100-W PEMFC stack. At beginning, power was increased gradually, then kept constant.

4. Conclusion

The Nafion membrane as an electrolyte plays an important role in the construction of a PEMFC's membrane electrode assembly (MEA). Various types of Nafion membranes, such as Nafion 117, 115, 112, and 105, were tested with a single cell at different temperatures. Nafion 112 gave the optimal result (0.72 V at 1.0 A/cm^2). A 30-cell stack (100 W) was evaluated at different humidity levels and temperatures. The potential-current and power-current curves for both the single cell and the stack were analyzed by computer simulation, and the kinetic and mass-transfer parameters were calculated. The values of open-circuit potential, Tafel slope, and dc resistance of the stack (cells linked in series) seem to correspond to the simple addition of the values of all single cells. However, the mass-transfer behavior is more complicated for the stack compared with that of the single cell because of the presence of more factors, such as heat exchange, humidity, and air and fuel supply. The long-term performance of the stack and the production of water during long-term operation were also measured. The stack system becomes more stable and reaches optimal performance after running several hours under constant current or constant power. The optimal performance is reached at about 170 W. Only 66 percent of the theoretical water was actually collected during long-term operation, while the other 34 percent of water was lost by evaporation. The system is self-humidifying, using the water produced by the cathode electrode. Self-humidification is more efficient at 30 °C than below 10 °C.

Acknowledgment

The authors wish to thank the U.S. Army Materiel Command for its financial support of this project.

References

1. T. F. Fuller, "Is a Fuel Cell in Your Future?" *The Electrochemical Society Interface* (Fall 1997), p 26.
2. E. A. Ticianelli, C. R. Derouin, and S. Srinivasan, "Localization of Platinum in Low Catalyst Loading Electrodes to Attain High Power Density in SPE Fuel Cells," *J. Electroanal. Chem.* **251** (1988), p 175.
3. I. D. Raistrick, "Electrode Assembly for Use in a Solid Polymer Electrolyte Fuel Cell," U.S. patent No. 4,876,115 (1990).
4. M. S. Wilson and S. Gottesfeld, "Thin-Film Catalysis Layers for Polymer Electrolyte Fuel Cell Electrodes," *J. Appl. Electrochem.* **22** (1992), pp 1–7.
5. J. Kim, S. M. Lee, S. Srinivasan, and C. E. Chamberlin, "Modeling of Proton Exchange Membrane Fuel Cell Performance with an Empirical Equation," *J. Electrochem. Soc.* **142** (1995), p 2670.
6. Y. W. Rho, O. A. Velev, S. Srinivasan, and Y. T. Kho, "Mass Transfer Phenomena in Proton Exchange Membrane Fuel Cells Using O_2/He, O_2/Ar, and O_2/N_2 Mixtures, I. Experimental Analysis," *J. Electrochem. Soc.* **141** (1994), p 2084.
7. H. F. OetJen, V. M. Schmidt, U. Stimming, and F. Trila, "Performance Data of a Proton Exchange Membrane Fuel Cell Using H_2/CO as Fuel Gas," *J. Electrochem. Soc.* **143** (1996), p 3838.
8. M. Uchida, Y. Aoyama, N. Eda, and A. Ohta, "Investigation of the Microstructure in the Catalyst Layer and Effects of Both Perfluorosulfonate Ionomer and PTFE-Loaded Carbon on the Catalyst Layer of Polymer Electrolyte Fuel Cells," *J. Electrochem. Soc.* **142** (1995), p 4143.
9. F. N. Buchi, B. Gupta, O. Haas, and G. G. Scherer, "Performance of Differently Cross-Linked, Partially Fluorinated Proton Exchange Membranes in Polymer Electrolyte Fuel Cells," *J. Electrochem. Soc.* **142** (1995), p 3044.
10. M. Uchida, Y. Aoyama, N. Eda, and A. Ohta, "New Preparation Method for Polymer-Electrolyte Fuel Cells," *J. Electrochem. Soc.* **142** (1995), p 463.
11. J. B. Lakeman and J. Cruickshank, "A Lightweight Ambient Air Breathing Fuel Cell Stack," *Proceedings of the 38th Power Sources Conference*, Cherry Hill, NJ (June 1998), p 420.
12. A. Cisar, O. J. Murphy, and E. Clarke, "Low-Cost, Lightweight, High Power Density PEM Fuel Cell Stack," *Proceedings of the 38th Power Sources Conference*, Cherry Hill, NJ (June 1998), p 424.
13. L. P. Jarvis and D. Chu, "The Electrochemical Performance of a 100-Watt Polymer Electrolyte Membrane Fuel Cells and Single Cells," *Proceedings of the 38th Power Sources Conference*, Cherry Hill, NJ (June 1998), p 428.
14. O. Polevaya and D. Bloomfield, "Performance Modeling in a Lightweight Fuel Cell Stack," *Proceedings of the 38th Power Sources Conference*, Cherry Hill, NJ (June 1998), p 416.

Distribution

Admnstr
Defns Techl Info Ctr
Attn DTIC-OCP
8725 John J Kingman Rd Ste 0944
FT Belvoir VA 22060-6218

Ofc of the Secy of Defns
Attn ODDRE (R&AT)
The Pentagon
Washington DC 20301-3080

OSD
Attn OUSD(A&T)/ODDR&E(R) R J Trew
Washington DC 20301-7100

Advry Grp on Elect Devices
Attn Documents
Crystal Sq 4 1745 Jefferson Davis Hwy Ste 500
Arlington VA 22202

AMCOM MRDEC
Attn AMSMI-RD W C McCorkle
Redstone Arsenal AL 35898-5240

CECOM
Attn PM GPS COL S Young
FT Monmouth NJ 07703

CECOM Night Vsn/Elect Sensors Dirctrt
Attn AMSEL-RD-NV-D
FT Belvoir VA 22060-5806

Commander
CECOM R&D
Attn AMSEL-IM-BM-I-L-R Stinfo Ofc
Attn AMSEL-IM-BM-I-L-R Techl Lib
FT Monmouth NJ 07703-5703

Deputy for Sci & Techlgy
Attn Ofc Asst Sec Army (R&D)
Washington DC 30210

Dir for MANPRINT
Ofc of the Deputy Chief of Staff for Prsnnl
Attn J Hiller
The Pentagon Rm 2C733
Washington DC 20301-0300

Hdqtrs
Attn DAMA-ARZ-D F D Verderame
Washington DC 20310

TECOM
Attn AMSTE-CL
Aberdeen Proving Ground MD 21005-5057

US Army Armament Rsrch Dev & Engrg Ctr
Attn AMSTA-AR-TD M Fisette
Bldg 1
Picatinny Arsenal NJ 07806-5000

Commander
US Army CECOM
Attn AMSEL-RD-CZ-PS-B M Brundage
FT Monmouth NJ 07703-5000

US Army CECOM Rsrch Dev & Engrg Ctr
Attn AMSEL-RD-AS-BE E Plichta
FT Monmouth NJ 07703-5703

US Army Edgewood RDEC
Attn SCBRD-TD G Resnick
Aberdeen Proving Ground MD 21010-5423

US Army Info Sys Engrg Cmnd
Attn ASQB-OTD F Jenia
FT Huachuca AZ 85613-5300

US Army Natick RDEC
Acting Techl Dir
Attn SSCNC-T P Brandler
Natick MA 01760-5002

US Army Simulation, Train, & Instrmntn Cmnd
Attn J Stahl
12350 Research Parkway
Orlando FL 32826-3726

US Army Tank-Automtv Cmnd Rsrch, Dev, & Engrg Ctr
Attn AMSTA-TA J Chapin
Warren MI 48397-5000

Distribution (cont'd)

US Army Train & Doctrine Cmnd
Battle Lab Integration & Techl Dirctrt
Attn ATCD-B J A Klevecz
FT Monroe VA 23651-5850

US Military Academy
Mathematical Sci Ctr of Excellence
Attn MDN-A LTC M D Phillips
Dept of Mathematical Sci Thayer Hall
West Point NY 10996-1786

Nav Rsrch Lab
Attn Code 2627
Washington DC 20375-5000

Nav Surface Warfare Ctr
Attn Code B07 J Pennella
17320 Dahlgren Rd Bldg 1470 Rm 1101
Dahlgren VA 22448-5100

Marine Corps Liaison Ofc
Attn AMSEL-LN-MC
FT Monmouth NJ 07703-5033

USAF Rome Lab Tech
Attn Corridor W Ste 262 RL SUL
26 Electr Pkwy Bldg 106
Griffiss AFB NY 13441-4514

DARPA
Attn S Welby
3701 N Fairfax Dr
Arlington VA 22203-1714

Hicks & Associates Inc
Attn G Singley III
1710 Goodrich Dr Ste 1300
McLean VA 22102

Palisades Inst for Rsrch Svc Inc
Attn E Carr
1745 Jefferson Davis Hwy Ste 500
Arlington VA 22202-3402

US Army Rsrch Lab
Attn AMSRL-RO-EN B Mann
Attn AMSRL-RO-EN Bach
Attn AMSRL-RO-D JCI Chang
PO Box 12211
Research Triangle Park NC 27709

US Army Rsrch Lab
Attn AMSRL-DD J Miller
Attn AMSRL-CI-AS Mail & Records Mgmt
Attn AMSRL-CI-AT Techl Pub (3 copies)
Attn AMSRL-CI-LL Techl Lib (3 copies)
Attn AMSRL-SE-D E Scannell
Attn AMSRL-SE-DC D Chu (30 copies)
Attn AMSRL-SE-DC S Gilman
Attn AMSRL-SE-E J Mait
Adelphi MD 20783-1197

REPORT DOCUMENTATION PAGE

Form Approved
OMB No. 0704-0188

1. AGENCY USE ONLY *(Leave blank)*	2. REPORT DATE	3. REPORT TYPE AND DATES COVERED
	February 2000	Progress, Oct. 1998 to Sept. 1999

4. TITLE AND SUBTITLE Comparative Studies of Polymer Electrolyte Membrane Fuel Cell Stacks and Single Cells

5. FUNDING NUMBERS
DA PR: N/A
PE: 62120A

6. AUTHOR(S) Deryn Chu and Rongzhong Jiang

7. PERFORMING ORGANIZATION NAME(S) AND ADDRESS(ES)
U.S. Army Research Laboratory
Attn: AMSRL-SE-DC email: dchu@arl.mil
2800 Powder Mill Road
Adelphi, MD 20783-1197

8. PERFORMING ORGANIZATION REPORT NUMBER
ARL-TR-2087

9. SPONSORING/MONITORING AGENCY NAME(S) AND ADDRESS(ES)
U.S. Army Research Laboratory
2800 Powder Mill Road
Adelphi, MD 20783-1197

10. SPONSORING/MONITORING AGENCY REPORT NUMBER

11. SUPPLEMENTARY NOTES
ARL PR: 9NV4VV
AMS code: 622120.H16

12a. DISTRIBUTION/AVAILABILITY STATEMENT Approved for public release; distribution unlimited.

12b. DISTRIBUTION CODE

13. ABSTRACT *(Maximum 200 words)*

We made a comparative investigation of a polymer electrolyte membrane fuel cell (PEMFC) with a single cell and a 30-cell stack. Various types of Nafion membranes, such as Nafion 102, 112, 115, and 117, and 105, were tested as electrolytes with the single cell at different temperatures. Nafion 112 gave us the optimal result. We evaluated the 30-cell stack at different temperatures and humidity levels. The potential-current and power-current curves for both the single cell and the stack were analyzed by computer simulation, during which the kinetic and mass-transfer parameters were calculated. We also measured the performance of the stack and its water production during long-term operation.

14. SUBJECT TERMS
Fuel cell, polymer membrane, Nafion

15. NUMBER OF PAGES
23

16. PRICE CODE

17. SECURITY CLASSIFICATION OF REPORT	18. SECURITY CLASSIFICATION OF THIS PAGE	19. SECURITY CLASSIFICATION OF ABSTRACT	20. LIMITATION OF ABSTRACT
Unclassified	Unclassified	Unclassified	UL

NSN 7540-01-280-5500

Standard Form 298 (Rev. 2-89)
Prescribed by ANSI Std. Z39-18
298-102